

Equilibrium and Nonequilibrium phase transitions in continuous symmetric classical magnets

Olivia Mallick and Muktish Acharyya

Department of Physics, Presidency University, Kolkata, India

Contents

1	Introduction:	4
2	Equilibrium phase transition in Continuous Symmetric Models:	5
2.1	Phase transition of the isotropic planar ferromagnet in equilibrium:	5
2.1.1	Classical calculations:	5
2.1.2	Quantum calculations:	5
2.2	Anisotropic planar ferromagnetic model:	5
2.2.1	Role of anisotropy in the ferromagnetic phase transition:	6
2.2.2	Layered XY antiferromagnet:	11
2.3	Heisenberg Model:	12
2.3.1	Ferromagnetic phase transition in Heisenberg model: A brief historical survey	12
2.3.2	Metamagnetic behaviour of anisotropic Heisenberg model: Experiment versus numerical sim	
3	Non equilibrium phase transition in Continuous Symmetric Models:	15
3.1	Planar ferromagnet perturbed by polarised magnetic field	15
3.1.1	Partial Transition in Symmetry Breaking Dynamics	16
3.1.2	Comprehensive Phase Boundary	19
3.2	Anisotropic Heisenberg Ferromagnet in External Magnetic Field	20
3.2.1	Longitudinal and transverse dynamic transition	21
3.2.2	Elliptically polarized magnetic field: Multiple dynamic transition	22
4	Technological significance:	29
5	Summary:	29
6	Acknowledgements:	30

arXiv:2309.04127v1 [cond-mat.stat-mech] 8 Sep 2023

Abstract: The magnetism is an old problem of Physics. Most interesting part of the research on magnetism is its thermodynamic behaviour. In this review, the thermodynamic phase transitions, mainly in ferromagnetic model systems, are discussed. The model system has a characteristic of continuous symmetry. In this context, the classical XY and Heisenberg model are chosen for discussion. With a historical survey of such phase transition observed in such models, the results of the recent (over two decades) studies are collected and reviewed. The equilibrium phase transition in such systems are discussed to highlight the dependence of the critical temperatures on the anisotropy, dilution etc. On the other hand, the nonequilibrium results of such systems driven by time dependent magnetic field, are also reviewed. We believe, this review is a modern documentation and collection of works in the field of theoretical magnetism which may be extremely useful for the researcher working in this field.

Keywords: Anisotropic system, Continuous symmetry, Ferromagnetic system, Metastable behaviour, Heisenberg model , Magnetic anisotropy, Metropolis protocol, Monte Carlo methods, Random anisotropy and disorder, XY ferromagnets

Objectives:

- To discuss the previous work in the field of magnetism.
- To focus to the equilibrium results of thermodynamics of magnetism.
- The model systems are considered as having the continuous symmetry.
- To discuss the equilibrium phase transition of XY and Heisenberg model.
- To discuss the nonequilibrium phase transition of XY and Heisenberg model.
- To discuss the relevant technological significances.

1 Introduction:

The magnetism in nature is an astonishing phenomenon. The material magnetism (apart from electromagnetism) has drawn the attention of the researcher over several decades. The experimental as well as theoretical science in the material magnetism are now a rich and well developed field of Physics literature.

Although, according to the Bohr-Van Leeuwen's theorem, the magnetism is a quantum phenomenon, many thermodynamic aspects of material magnets can be well described by classical models. The classical models deal with vector (spin) which can assume any direction (generally forbidden by quantum mechanics). However, such kind of classical model of planar (two dimensional vector) ferromagnet in two dimensions can give rise [Kosterlitz, 1974] to interesting ordered phase even in the absence of long range ferromagnetic order. Such a phase, celebrated Kosterlitz-Thouless phase, shows vortices (pairwise vortex-antivortex) below a certain critical temperature. This discovery of the topological phases has received Nobel prize in 2016.

The most general model of magnetic system is Heisenberg model. The thermodynamic behaviours of the ferromagnetism, antiferromagnetism, metamagnetism, canted phases, spin-glass phase all are well explained by Heisenberg model. The anisotropy plays an important role in the transition temperature of the critical phenomena. This anisotropy breaks the special orthogonal symmetry in the planar magnetic (XY) model and $SO(3)$ symmetry in the Heisenberg model. A huge literature has been developed, over last several decades, regarding the phase transitions in anisotropic XY and anisotropic Heisenberg ferromagnet. In the anisotropic planar (XY) magnet, these anisotropy in the system can be implemented in various ways. However, in the case of Heisenberg magnet, the single site anisotropic models are investigated. The constant anisotropic as well as distributed anisotropic planar ferromagnetic phase (equilibrium type) transitions are studied recently and discussed in this article.

In this review article, we mainly discussed the thermodynamic properties of these two (XY and Heisenberg) models. Moreover, these models, driven by the time varying external magnetic field, give rise to the nonequilibrium phase transitions. The externally applied time varying magnetic field may be represented in different ways. The first kind of time dependence is the sinusoidally oscillating (in time but uniform over the space) magnetic field. This time dependence keeps the system away from the equilibrium. As a result, the system undergoes a nonequilibrium kind of phase transition. The nonequilibrium phase transition in Heisenberg magnet has been discussed. Another kind of time dependence may arise when the electromagnetic wave passes through the magnetic sample. The spatio-temporal variations of magnetic field wave (the interacting part of the wave) may also give rise to nonequilibrium phase transition. We have also discussed the interesting results of such nonequilibrium behaviours.

The whole manuscript has been organized as follows: The section-2 is devoted to the phase transition of the spin models having continuous symmetric. Section-3 contains the discussion on nonequilibrium phase transition in spin models described by the continuous symmetry. The technological significance is discussed in section-4. The manuscript end with some concluding remarks in section-5.

2 Equilibrium phase transition in Continuous Symmetric Models:

In this section, we will discuss the phase transition in equilibrium observed in planar ferromagnetic (XY) model and Heisenberg model.

2.1 Phase transition of the isotropic planar ferromagnet in equilibrium:

2.1.1 Classical calculations:

In this subsection will discuss only the ferromagnetic phase transition (of classical rotor) in three dimensional XY ferromagnetic system. We will not discuss here the spin vortex related KT transition in two dimensional planar ferromagnet. The system is described by the following spin Hamiltonian:

$$\mathcal{H} = -J \sum_{ij} \sigma_{ix} \sigma_{jx} + \sigma_{iy} \sigma_{jy} \quad (1)$$

This kind of Hamiltonian is not exactly solvable and hence recent Monte Carlo studies [Campostrini et al., are referred here to get the numerical estimates of the critical temperature and the critical exponents. [Hasenbusch, 2008] has estimated the critical temperature $kT_c/J = 2.206$ through extensive Monte Carlo simulations. [Campostrini et al., 2001] reported the Monte Carlo estimates of the critical exponents as $\alpha = 0.0146(8)$, $\beta = 0.3485(2)$, $\gamma = 1.3177(5)$, $\delta = 4.780(2)$, $\nu = 0.67155(27)$ and $\eta = 0.0380(4)$. These set of values of the critical exponents defines the universality class of three dimensional XY ferromagnet. The domain growth and aging in planar ferromagnet has been studied recently [Agrawal et al., 2021], in the presence of random field.

2.1.2 Quantum calculations:

It may be noted here that a quantum version of XY ferromagnet (of spin-1/2) has been investigated [Betts and Lee, 1968] where the Hamiltonian is represented as $\mathcal{H} = -J \sum_{ij} \sigma_{ix} \sigma_{jx} + \sigma_{iy} \sigma_{jy} = -J \sum_{ij} a_i^\dagger a_j + a_i a_j^\dagger$, where $\vec{\sigma}$ is Pauli spin matrices and a , a^\dagger are corresponding field operators coming via Jordan-Wigner transformation. The transition temperature $kT_c/J \approx 4.84$ and the critical exponents $\gamma \approx 1.00$ and $\alpha \approx 0.02$ are estimated for face centred cubic lattice. Where γ and α are the critical exponents for the susceptibility and the specific heat respectively.

2.2 Anisotropic planar ferromagnetic model:

The magnetic anisotropy in the planar (XY) ferromagnet plays an important role in its phase. The vortex loop scaling has been studied [Shenoy and Chattopadhyay, 1995] in three dimensional anisotropic XY model. The quantum nature of the critical behaviour of anisotropic spin-1/2 planar model ferromagnet has been studied Su et al., 2022 with staggered Dzyaloshinskii-Moriya kind of interaction. Geometrically frustrated XY models has been investigated [Lach and Žukovič, 2020] to have the emergent new kind of phase. The antiferromagnetic phases in planar (XY) ferromagnetic model on a triangular lattice with interactions of higher order, is also reported [Lach and Žukovič, 2021], recently. Let us now report recent results on the phase transition in three dimensional classical anisotropic XY ferromagnet.

The anisotropic XY ferromagnet system described by the following kind of Hamiltonian:

$$\mathcal{H} = -J \sum_{\langle i,j \rangle} (1 + \gamma_{ij}) \sigma_i^x \sigma_j^x + (1 - \gamma_{ij}) \sigma_i^y \sigma_j^y \quad (2)$$

where $\sigma_i^x (= \cos\theta_i)$ and $\sigma_i^y (= \sin\theta_i)$ represent the components of the two dimensional vector (put in the i-th lattice position) having the magnitude unity, $|\sigma|=1$. θ represents the directional angle of orientation of the spin vector. Classically, θ may assume any value between 0 and 2π . The anisotropy is modelled by the parameter γ_{ij} . The system restores isotropicity or conventional XY for $\gamma_{ij} = 0$, and for $\gamma_{ij} = 1$ the system maps to ferromagnetic XX model. The nearest neighbour ferromagnetic interaction strength is represented by $J(> 0)$. The anisotropy significantly governs the behaviour of magnetic systems. It would be fascinating to study the thermodynamic behaviours of the XY ferromagnet for constant (over the lattice) anisotropy as well as for distributed anisotropy. Here, we discuss the recent results for three different kinds of randomly (uniform, bimodal and Gaussian) distributed anisotropies [Mallick and Acharyya, 2023].

a) *Uniform distribution*: The distribution of random anisotropy is uniform.

$$P_u(\gamma_{ij}) = \frac{1}{\omega}, \quad (3)$$

here ω stands for the characteristic spread of the statistical distribution. The values of the anisotropy are randomly quenched over each lattice position. The anisotropy may assume the values randomly within domain specified between $-\omega/2$ and $+\omega/2$. The variable $\sigma_u = \frac{\omega}{2\sqrt{3}}$ is the, variance raised to the power 1/2, of the probability density function (PDF). Hence the statistical standard deviation(σ_u) is connected to the spread of the probability distribution function of the random anisotropy(γ_{ij}).

b) *Gaussian or Normal distribution*: The random anisotropy is distributed by Gaussian formula,

$$P_n(\gamma_{ij}) = \frac{1}{\sqrt{2\pi\omega}} e^{-\frac{\gamma_{ij}^2}{2\omega^2}}. \quad (4)$$

The widely used Box Muellar algorithm has been employed to generate such Gaussian or Normal distribution. Here ω , represents the width of the distribution. The standard deviation is denoted by $\sigma_n (= \omega)$. It may be noted here that only for this particular kind of distribution (Gaussian) the width and standard deviation are equal.

c) *Bimodal Distribution*: The random anisotropy follows a bimodal kind of distribution

$$P_b(\gamma_{ij}) = \frac{1}{2} [\delta(\gamma_{ij} - \frac{\omega}{2}) + \delta(\gamma_{ij} + \frac{\omega}{2})]. \quad (5)$$

here δ is the Dirac Delta function. Here, the values of the anisotropy, $-\omega/2$ or $+\omega/2$, are equally probable. The standard deviation (σ_b) and the width of the distribution (ω) are related as $\sigma_b = \frac{\omega}{2}$. The mean value of anisotropy $\langle \gamma_{ij} \rangle = 0$ for all distributions mentioned above.

2.2.1 Role of anisotropy in the ferromagnetic phase transition:

The extensive Monte Carlo (MC) simulations have been performed [Mallick and Acharyya, 2023] in three dimensional classical anisotropic XY ferromagnet using Metropolis algorithm. For constant anisotropy, the MC estimate of the pseudocritical temperature has shown a linear increase with the strength of constant anisotropy (Fig-1) whereas nonlinear decrease of pseudocritical temperature has been noticed (Fig-2) for the distributed anisotropies. The reduction of pseudocritical temperature

for distributed anisotropy may be realized just by considering the randomly quenched anisotropy as disorder. The disorder definitely reduces the critical temperature. Whereas, the constant anisotropy increases the critical temperature. The constant anisotropy just breaks the $SO(2)$ symmetry in the system which is responsible for increasing the pseudocritical temperature. All these critical behaviours are formalized by the analysis of size dependence assuming the scaling behaviours, for the magnetisation and the susceptibility. The critical exponents ($\frac{\beta}{\nu}$ and $\frac{\gamma}{\nu}$) are evaluated (Mallick and Acharyya, 2023).

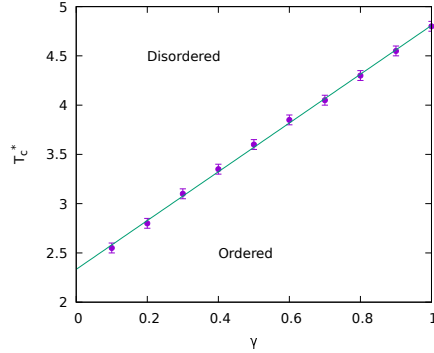


Figure 1: The finite sized transition temperature (T_c^*) is shown as a function of the magnitude of anisotropy (γ). Here, γ is constant over the lattice. Collected from [Mallick and Acharyya, 2023]

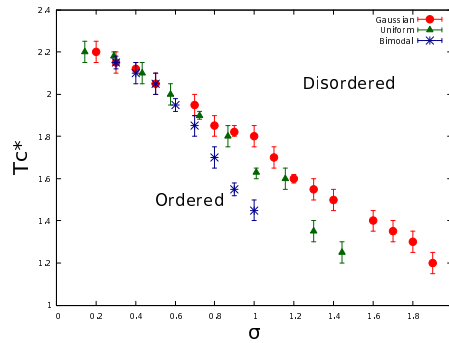


Figure 2: The finite system's transition temperature (T_c^*) is depicted as the function of the standard deviations of the various types of probability density functions of the random anisotropy (γ_{ij}): Uniform(Green triangle), Gaussian(Red bullet), Bimodal(Blue star). The errorbars represent the maximum error involved in determining T_c^* . Collected from [Mallick and Acharyya, 2023]

What kind of critical behaviour is expected from disordered (quenched) XY ferromagnet ? The disordered planar ferromagnet can be modelled by three dimensional XY model with randomly quenched nonmagnetic impurity with a specified concentration. The site diluted classical XY ferromagnet has been studied [Santos-Filho and Plascak, 2011] by Monte Carlo simulation. The ordered ferromagnetic to disordered paramagnetic phase transformation has been found to occur at lower temperature for nonzero impurity concentration. The pseudocritical temperature has been studied as function of the concentration of magnetic sites and the results are compared with that for experimental results. The following figure shows the results:

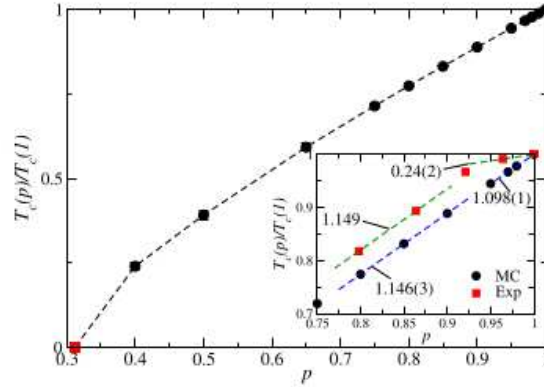


Figure 3: The effects of nonmagnetic quenched impurity on the transition temperature. The transition temperature is plotted against the concentration of magnetic sites. The percolation threshold is marked by square. The dashed line is just joining the data points. The experimental results from [DeFotis et al., 2008] are compared and shown in the inset is the for low concentrations. Collected from [Santos-Filho and Plascak, 2011]

However, a recent Monte Carlo study [Mallick and Acharyya, 2022] reports the linear variation of the pseudocritical temperature with the impurity concentration of three dimensional site diluted XY ferromagnet. The results are depicted in Fig-4.

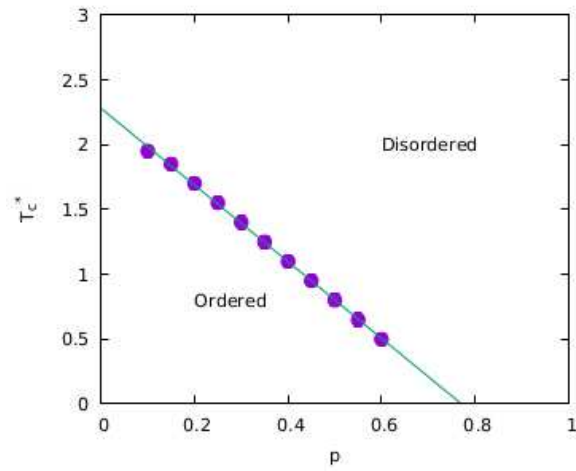


Figure 4: The pseudocritical temperature T_c^* is plotted against the concentration p of nonmagnetic impurity in a three dimensional XY ferromagnet. Collected from [Mallick and Acharyya, 2022]

The anisotropic XY ferromagnet has been treated quantum mechanically to obtain the critical temperature as function of anisotropy. The T_c has been calculated from magnonic dispersion relation as $T_c = \frac{4dJ}{I(0)+I(D/dJ)}$, where D is the strength of single site anisotropy and the function $I(x)$ is standard extended Watson integral [Zucker, 2011] The following figure (Fig-5 shows the results and the line separating the regions of ferromagnetic and paramagnetic phases. Collected from, [Ma and Figueiredo, 1997]. The nonlinear variation in such quantum calculation is significantly different from the linear variation in the recent MC estimates [Mallick and Acharyya, 2022]. The possible reason may be the nature of anisotropy considered in the later case.

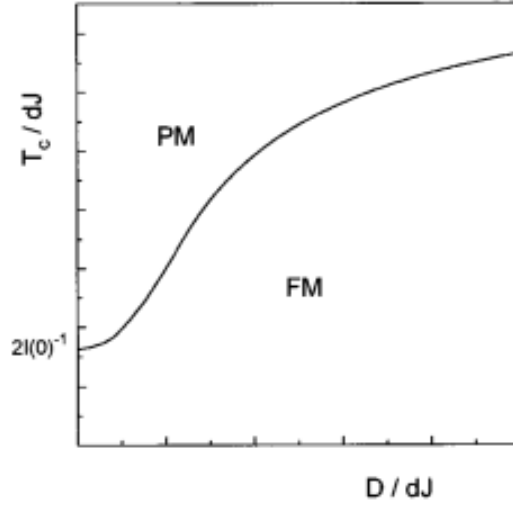


Figure 5: The dependence of the thermal critical point T_c on the strength of single site anisotropy D . Collected from [Ma and Figueiredo, 1997]

2.2.2 Layered XY antiferromagnet:

So far, we have discussed the critical behaviours of anisotropic XY ferromagnet. In this section the equilibrium thermodynamic behaviour of the layered XY antiferromagnet will be discussed by considering both (ferromagnetic and antiferromagnetic) kinds of interaction in the XY model. As a prototype, the layered XY antiferromagnet (or XY metamagnet) has been studied [Acharyya and Vatansever, 2022].

The following Hamiltonian represents the XY metamagnet:

$$H = -J_f \sum_{\text{intra-planar}} (\sigma_i^x \sigma_j^x + \sigma_i^y \sigma_j^y) - J_a \sum_{\text{inter-planar}} (\sigma_i^x \sigma_j^x + \sigma_i^y \sigma_j^y) - \sum_i (h_x \sigma_i^x + h_y \sigma_i^y). \quad (6)$$

The ferromagnetic nearest neighbour interaction strength within a specific plane is denoted by $J_f (> 0)$. To introduce the anisotropy, the antiferromagnetic interaction strength $J_a (< 0)$ is considered between two adjacent planes. Here, the measure of relative interactions can be the ratio (R) of the interaction strengths $R = -\frac{J_a}{J_f}$. The h_x and h_y (measured in the unit of J_f) are the horizontal (x) and vertical (y) components of the magnetic fields (applied externally) respectively. We have applied the periodic (PBC) or closed conditions of the boundaries in the all of the three spatial directions.

The equilibrium thermodynamic behaviours of such system has been investigated by MC numerical simulation using Metropolis rule. The system has been found to show the equilibrium phase transition. The finite sized transition temperature has been observed to depend on the value of h_x (we have set $h_y = 0$) and R . The finite sized transition temperature has been predicted and evaluated by fixing the location of the maximum of the corresponding fluctuations of the order parameter. Fig-6 shows the phase separating boundaries in the $h_x - T_c$ plane for different values of R . This thermodynamic phase transition has been formalized [Acharyya and Vatansever, 2022] by finite size analysis.

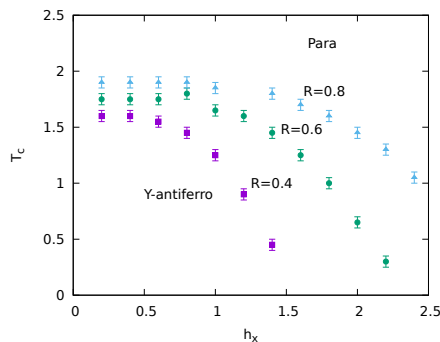


Figure 6: The phase separating lines for different values of R of the layered planar antiferromagnet. Collected from [Acharyya and Vatansever, 2022]

2.3 Heisenberg Model:

2.3.1 Ferromagnetic phase transition in Heisenberg model: A brief historical survey

The Heisenberg model is a good candidate to study the ferromagnetic phase transition. Historically, in 1969 the thermodynamic properties of two dimensional Heisenberg ferromagnet (spin-1/2) has been analysed [Mubayi and Lange, 1969] by Green function technique. The analysis predicted a phase transition at critical temperature $T_c = 2J/k$. The susceptibility was found to diverge at T_c . However, the vanishing long range ferromagnetic ordering has been observed (as predicted by [Stanley and Kaplan, 1966]) in all (both below and above the critical temperature) which is consistent with Mermin and Wagner theorem (absence of long range ferromagnetic order in continuous symmetric ferromagnetic models below three dimension).

After a few years [Oguchi, 1971], the ferromagnetic phase transition, for a general spin- S two dimensional Heisenberg model has been reported. The variational theory predicted a phase transformation with transition temperature (T_r) given by $kT_r = (2\sigma(\sigma + 1)/3)qJ$, where σ is the magnitude of spin, J is the ferromagnetic interaction strength and q is the coordination numbers. As the system cools down to the transition temperature T_r from higher temperature, the usual static susceptibility has been found to diverge as $(T - T_r)^{-1}$. However, the long range ferromagnetic order is found to be zero at all finite temperatures and for all spin values. This preserves the the celebrated Mermin Wagner criterion.

Later, the researchers have paid the intense attention to investigate the effects of anisotropy in the ferromagnetic behaviours of Heisenberg kind of systems. The readers may be referred a review article [Flax, 1970] for a theoretical understanding of anisotropic Heisenberg model. Let us briefly mention a few of the important results of such studies. Historically, Landau and Binder [Binder and Landau, 1976] reported the first Monte Carlo results of the critical properties of a two dimensional *anisotropic* Heisenberg ferromagnet. The anisotropy (Δ) has been introduced through the following Hamiltonian

$$H = -J \sum [(1 - \Delta)(\sigma_i^x \sigma_j^x + \sigma_i^y \sigma_j^y) + \sigma_i^z \sigma_j^z]. \quad (7)$$

The existence of nonzero spontaneous magnetisation at low temperature was first reported [Fröhlich and Lieb, 1977] in two dimensional anisotropic nearest neighbour Heisenberg ferromagnet. The existence of nonzero spontaneous magnetisation at low temperature, has been concluded, as due to the presence of anisotropy.

The Monte Carlo results provided the anisotropy dependent transition temperature. The transition temperature was found to exceed the value of critical temperature predicted for isotropic case by the method of series expansion.

The Monte Carlo simulations were performed (with improved algorithm) ([Serena et al., 1993] to study the two dimensional anisotropic Heisenberg model. The anisotropy dependent critical temperature has been shown in Fig-7. The validity of spinwave analysis was found in good agreement upto the temperature $T = 0.5T_c$.

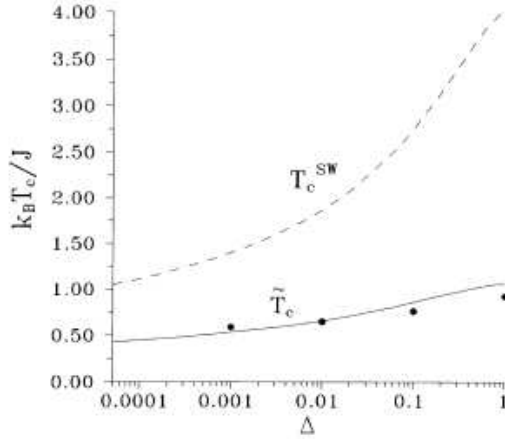


Figure 7: Critical Temperature versus anisotropy in two dimensional Heisenberg model. The spin-wave critical temperature is indicated by dashed line. Collected from [Serena et al., 1993]

The ultrathin magnetic film can be the realistic example of anisotropic Heisenberg ferromagnet. This has been shown [Rapini et al., 2007] in anisotropic Heisenberg model with long range interaction investigated by extensive Monte Carlo simulations. Three distinctly different phases are identified: Namely, a ferromagnetically ordered phase, a phase characterized by a change from out-of-plane to in-plane in the magnetization, and obviously a high-temperature paramagnetic or disordered phase.

The spin-rotation-invariant Green function theory was developed [Siurakshina et al., 2000] to analyse the behaviour of spatially anisotropic Heisenberg antiferromagnet and reported good agreement with the experimental results in La_2CuO_4 sample.

The extensive Monte Carlo simulation (with Metropolis and Wolff algorithm) has been employed to study [Freire and Plascak, 2015] the bicritical properties of three dimensional classical Heisenberg ferromagnet with single-site anisotropy subjected to crystal field. The bicritical point, has been concluded, to belong to the three dimensional Heisenberg universality class.

2.3.2 Metamagnetic behaviour of anisotropic Heisenberg model: Experiment versus numerical simulation

The FeBr_2 metamagnet shows many interesting phases. Experimentally observed, field induced transverse spin ordering [Petracic et al., 1998], has drawn the attention of theoretical researchers and prompted to visualize the effects in layered Heisenberg antiferromagnet or simply the Heisenberg metamagnet.

The continuous symmetric, Heisenberg model (with anisotropy) having competing type of spin-spin interactions exposed to an externally applied uniform magnetic field can be represented [Acharyya et al., 2000] by the energy function

$$H = -J \sum_{\langle ij \rangle} \vec{\sigma}_i \cdot \vec{\sigma}_j - J' \sum_{\langle ij \rangle'} \vec{\sigma}_i \cdot \vec{\sigma}_j - D \sum_i (\sigma_i^z)^2 - \vec{H} \cdot \sum_i \vec{\sigma}_i, \quad (8)$$

where the $\vec{\sigma}_i$ is representing a classical spin vector. This spin vector may assume any direction (classical picture). For simplicity, the system has been chosen as simple cubic type of lattice of linear size L . The interaction strengths $J > 0$ and $J' < 0$ represent the intra-planar ferromagnetic and

inter-planar antiferromagnetic interactions respectively. D is uniaxial anisotropy and \vec{H} represents the magnetic field applied externally. Here also, the standard PBC were applied as the boundary conditions in all three Euclidian directions.

A small amount of the transversely directed externally applied magnetic field ($H_x = 0.10$) has been applied additionally with the longitudinal field ($H_z = 0.70$) to mimic the experimental set up [Petracic et al., 1998]. Whereas, in real experiments [Petracic et al., 1998], the application of orthogonal (transverse) field is experimentally realized by obliquely keeping the FeBr_2 metamagnetic material by a small angle measured from the direction of applied magnetic field. The specific heat, studied experimentally, as a function of the temperature shows two distinct peaks. These two peaks indicate two distinct phase transitions. Theoretically, [Acharyya et al., 2000] the same scenario has been observed in Monte Carlo simulations, as an evidence of the fair agreement with the experimental results. Fig-8 shows the Monte Carlo results of the thermal variation of specific heat of Heisenberg metamagnet.

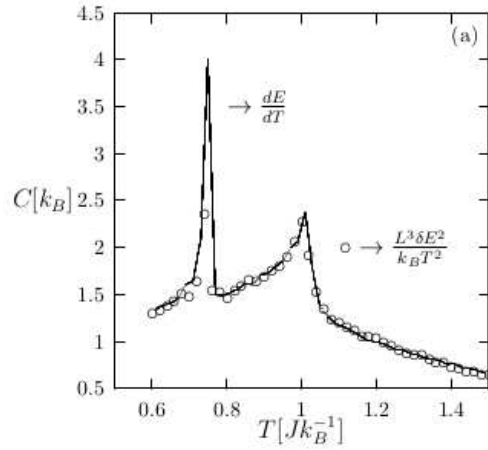


Figure 8: The specific heat of layered Heisenberg antiferromagnet. Collected from [Acharyya et al., 2000]

Let us briefly mention the interesting findings of some related studies on Heisenberg model. It may be mentioned here that recent quantum Monte Carlo study [Kanbur et al., 2020a] the thermodynamic properties of a two-leg rung-disordered ladder system shows the existence of a very special insensitive to the disorder strengths for the specific heat and the susceptibility.

The three dimensional quantum random bond Heisenberg antiferromagnet was found [Kanbur et al., 2020b] to be a member of three dimensional classical $O(3)$ symmetric universality class.

The classical Heisenberg model has been used to study [Akgenc et al., 2021] the magnetic phase transition in two dimensional Chromium based Janus MXenes. Recently, the two dimensional classical Heisenberg model has been employed to analyse [Bilican et al., 2023] the strain effects on

the electronic and magnetic properties of Cr_2TaC_2 and $\text{Cr}_2\text{TaC}_2\text{O}_2$ monolayers with reasonable agreement with the simulations results.

The recent Monte Carlo study [Naskar et al., 2023] reported the increase in the critical temperature, as the intensity of the single site anisotropy of classical three dimensional anisotropic Heisenberg ferromagnet, increased.

3 Non equilibrium phase transition in Continuous Symmetric Models:

Non-equilibrium ferromagnetic phase transitions occur in systems far from thermal equilibrium, where the dynamics of the system play a crucial role in determining its macroscopic behavior. Unlike equilibrium phase transitions, where the system evolves towards thermal equilibrium, non-equilibrium phase transitions occur in systems driven by external forces or subjected to time-dependent perturbations. These transitions often exhibit novel and intriguing phenomena due to the interplay between dynamics, fluctuations, and symmetry-breaking. The study of non-equilibrium ferromagnetic phase transitions in continuous symmetric models provides insights into various aspects of out-of-equilibrium statistical physics. In continuous symmetric models, the order parameter characterizing the ferromagnetic phase transition is typically a magnetization vector. This vector describes the alignment of magnetic moments in the system, which can exhibit spontaneous symmetry breaking when the temperature or other control parameters cross a critical value. In this context, investigating the breaking of dynamical symmetry in continuous symmetric models during non-equilibrium ferromagnetic phase transitions is of particular interest. This phenomenon reveals how the system's dynamics affect the symmetry properties and collective behavior, offering valuable insights into the underlying physics.

3.1 Planar ferromagnet perturbed by polarised magnetic field

The Hamiltonian of a planar ferromagnet can be expressed by incorporating a time-varying magnetic field that exhibits both spatial and temporal fluctuations:

$$\mathcal{H}(t) = -J \sum_{\langle ij \rangle} \sigma_i^x \sigma_j^x + \sigma_i^y \sigma_j^y - \sum_i \vec{h}_i(r, t) \cdot \vec{\sigma}_i \quad (9)$$

where $J > 0$ represents the strength of the exchange interaction between nearest neighboring magnetic moments, σ_i^x and σ_i^y denote the x and y components of the spin at site i, $\vec{h}_i(t)$ is the time-varying magnetic field at site i. The initial component of the Hamiltonian represents the interaction between adjacent spins, promoting alignment in the xy-plane and exhibiting ferromagnetic behavior. The second term accounts for the time varying magnetic field and magnetic moments at each site. The applied magnetic field exhibits both propagating and standing wave forms, characterized by their spatio-temporal variations. The propagating wave $h(r, t) = H \cos [2\pi(ft - z/\lambda)]$ is linearly polarized through the x-direction and propagates through the z-direction with its magnitude H . The standing wave has the form $h(r, t) = H \sin(2\pi ft) \sin(2\pi z/\lambda)$ oscillating along the z-direction with the same magnitude H and polarized in the x-direction. The framework is based on a three dimensional cubic lattice. The lattice has periodic boundary conditions, ensuring that spins at the edges of the lattice interact with their neighboring spins on the opposite side.

MC based numerical calculation is exploited to investigate the system's behaviour [Acharyya, 2018]. The nonequilibrium order parameter (\vec{Q}) components are, $Q_\alpha = \frac{1}{\tau} \oint M_\alpha(t) dt$. Where $M_\alpha(t) = \frac{1}{L^3} \sum \sigma_\alpha(r, t)$. are the instantaneous components of magnetisations and frequency $f = \frac{1}{\tau} = 0.01$ taken. The variances of Q_α (for α -th component) are defined as $Var(Q_\alpha) = L^3(\langle Q_\alpha^2 \rangle - \langle Q_\alpha \rangle^2)$. The non-equilibrium specific heat is expressed as $C = \frac{dE}{dT}$, where $E = \frac{1}{\tau} \oint H(t) dt$ corresponds to the time averaged energy across every phase of magnetic field cycle.

3.1.1 Partial Transition in Symmetry Breaking Dynamics

A three dimensional XY planner ferromagnet exposed to a *propagating or travelling* magnetic field wave with linear polarization reveals two exclusive phases that are influenced by temperature (T) and the strength of the magnetic field (H). At low temperatures, the XY ferromagnet exhibits a phase characterized by the phase-locked motion of spin-strips aligned with the direction of the magnetic field wave propagation (z-direction). The horizontal component of the spin, on an average, turns into zero under the influence of linearly polarized magnetic field wave through the horizontal direction. Nevertheless, the vertical component of the spin persists nonzero on average. In contrast, at high temperatures, the spin configurations become random and structureless, resulting in both the x and y components averaging to zero. To visualize the propagating spin mode, the y-component of the instantaneous planar magnetization is calculated for each XY plane as $PM_y(k) = \frac{1}{L^2} \sum \sigma_y$. The planar magnetization $PM_y(k)$ is plotted against the index k, which represents different XY planes, at two different times. The plotted data, shown in Figure 9(a), clearly demonstrates the presence of the propagating mode.

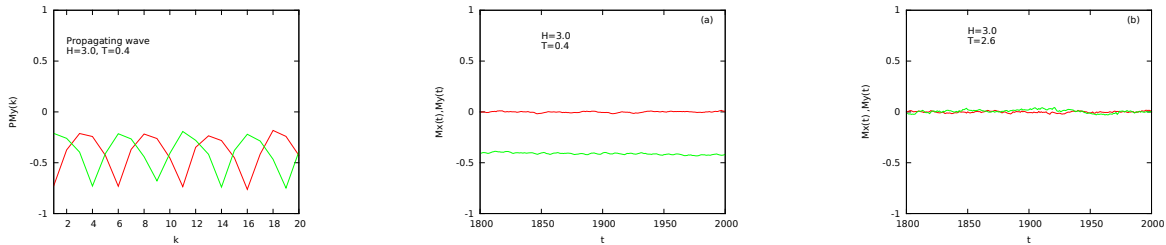


Figure 9: (a) The planar magnetization's y-component, $PM_y(k)$, is depicted against the XY plane indexed by k . distinct colours indicate distinct time instants: red corresponds to 1900th MCSS and green corresponds to 1930th MCSS. The wave moves in the z-direction. Temporal evolution of the horizontal (red) and vertical (green) magnetisation components (b) at low temperature $T = 0.40J/k_B$ (symmetry broken phase) (c) at high temperature $T = 2.60J/k_B$ (symmetric phase) at $H = 3.0J$, $f = 0.01(MCSS)^{-1}$ and $\lambda = 10$. The diagrams illustrate the infringement of dynamical symmetry (partial, only along y direction) in circumstance of propagating magnetic field. Collected from [Acharyya, 2018]

The statistical distributions of spin orientation, expressed by $\phi = \tan^{-1} \left(\frac{\sigma_y}{\sigma_x} \right)$, at a particular time, reveal the dynamically resilient spin configurations in response to a propagating magnetic field wave. At sufficiently low temperature the distribution has three modes at $\phi = 0^\circ$, $\phi \approx 180^\circ$ and $\phi \approx 360^\circ$. At $\phi = 90^\circ$, the distribution vanishes. Near $\phi = 270^\circ$, the distribution becomes non-zero. The distribution of angles observed confirms the existence of a predominantly y-component

in the spins, while the x-component is almost negligible. In contrast, the structureless spin arrangement at elevated temperature ($T = 2.60J/k_B$) is certified by the statistically distributed spin angles having three modes of equal weightage ([Acharyya, 2018]).

The temporal variation of the magnetization components $M_x(t)$ and $M_y(t)$ are depicted for two temperature regime in Figure 9(b) and (c) respectively. At sufficiently low temperature regime ($T = 0.40J/k_B$), the x-component of the instantaneous magnetization, denoted as $M_x(t)$, remains near zero with slight fluctuations. Conversely, the y-component, represented as $M_y(t)$, displays a non-zero value accompanied by fluctuations. In contrast, at higher temperatures ($T = 2.60J/k_B$), both components exhibit oscillations around zero without any appreciable deflection.

During the cooling process from high temperature, the system encounters a breaking of dynamical symmetry partially, manifested through the behavior of the y-component of magnetization ($M_y(t)$). As the system undergoes cooling, the dynamic order parameter Q_y encounters a transition from zero, indicating a phase of dynamic symmetry and disorder, to a non-zero value, indicating a phase of dynamic symmetry breaking and order. This transition temperature, known as the dynamic transition temperature, marks the critical point below which Q_y becomes non-zero. As the maximum value (H) of the travelling field wave increases, the nonequilibrium transition temperature shows a decreasing pattern. Overall, these findings highlight the dependence of the nonequilibrium transition temperature on the maximum value of the travelling field wave, as confirmed by the variance of Q_y and the behavior of the nonequilibrium specific heat C .

It is worth mentioning that the dynamical symmetry breaking has been verified experimentally by [Riego et al., 2017]. The decaying behaviour of the nonequilibrium ordered phase has also been studied experimentally in uniaxial cobalt film by [Berger et al., 2013].

(b) *Standing wave:*

The XY ferromagnet, when subjected to a stationary magnetic field wave, displays two distinct dynamic phases that are influenced by both temperature (T) and the maximum value (H) of the field. The spin configurations are analysed in the plane formed by X and Z axes at $Y=10$ and $H=3.0$, under conditions of cold thermal condition ($T = 0.40J/k_B$) and hot thermal conditions ($T = 2.60J/k_B$). At low temperatures, a standing spin wave mode is observed, characterized by stationary spin bands. An alternative visualization of the stationary mode in an induced spin wave within the XY ferromagnet involves plotting the y-component of the planar magnetization, denoted as $PM_y(k)$, as a function of the index k for the k -th XY plane. Figure 10(a) displays these plots for two distinct time instances. In the case of standing magnetic field wave, the k dependence of $PM_y(k)$ remain unchanged in their corresponding position over time, in contrast to the behavior observed in the propagating mode.

The probability distribution function of the angles (spin vector) shows four peaks near $\phi = 0^\circ$, slightly above $\phi = 0^\circ$, slightly below $\phi = 180^\circ$, and around $\phi = 270^\circ$. This tetramodal distribution leads to an overall negative y-component of magnetization, with an average x-component of magnetization of zero. This represents a dynamically ordered phase with partial symmetry breaking in the y-component. At high temperatures, the spin configuration appears random and structureless. The statistical distribution of spin vector angles exhibits a symmetric and trimodal shape with peaks near $\phi = 0^\circ, \phi = 180^\circ$ and $\phi = 360^\circ$ of approximately equal height. This results in a vanishing net y-component of magnetization and an average x-component of magnetization of zero, representing a dynamically disordered phase.

The presence of a partially symmetry broken ordered phase at low temperatures and a symmetric phase at high temperatures in the XY ferromagnet driven by a standing wave is evident from the observations. The time-varying dynamics of the magnetization components clearly reveal the viola-

tion of dynamical symmetry. By examining the instantaneous horizontal and vertical components of the magnetisation as time-varying function, shown in Figure 10(b) and (c), distinct characteristics of the higher temperature ($T = 2.60J/k_B$) and lower temperature ($T = 0.40J/k_B$) phases become apparent. In the high temperature phase, a dynamically symmetric state is observed, with both horizontal and vertical components of the magnetisation varying around the zero value with almost equal importance. Conversely, in the cold thermal state, a partial breaking of symmetry is observed, specifically in the y-component $My(t)$, which exhibits an asymmetric variation around the zero line. These findings suggest the occurrence of a symmetry broken nonequilibrium transition in the perturbed planar ferromagnet under the influence of a standing/stationary magnetic wave. Importantly, in both of the nonequilibrium phases, the mean horizontal component of the magnetization over a complete cycle of the standing wave, is precisely zero.

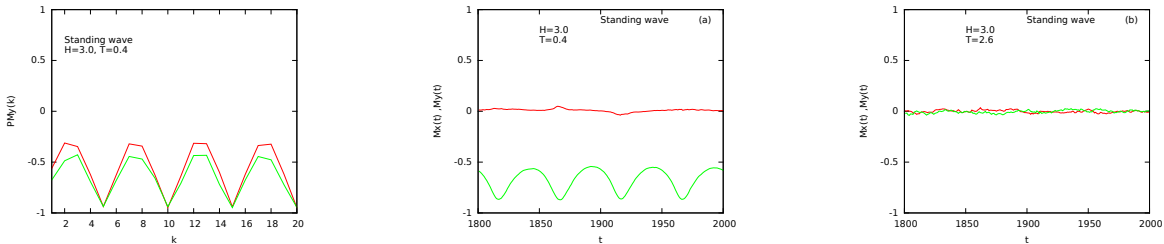


Figure 10: (a) The planar magnetization’s y-component, $PMy(k)$, is depicted against the XY plane indexed by k . distinct colours indicate distinct time instants: red corresponds to 1900th MCSS and green corresponds to 1930th MCSS. The wave moves in the z -direction. Temporal evolution of horizontal (red) and vertical (green) components of the magnetisation (b) at low temperature regime $T = 0.40J/K_B$ (broken-symmetric phase) (c) at high temperature regime $T = 2.60J/K_B$ (phase with symmetry) at $H = 3.00J$, $f = 0.01(MCSS)^{-1}$ and $\lambda = 10$. The diagrams illustrate the infringement of dynamical symmetry (partial, only along y direction) in circumstance of standing magnetic field. Collected from [Acharyya, 2018]

To explore the nonequilibrium transition related to the symmetry destructing in a perturbed planar ferromagnet, the thermal variations of Q_y , $Var(Q_y)$, and C were evaluated. The results revealed interesting behaviors. As the system undergoes a cooling process starting from elevated temperatures, Q_y exhibited a nonzero value near a transition temperature. Notably, this transition temperature decreased with increasing values of the applied field amplitude H . Furthermore, sharp peaks were observed in $Var(Q_y)$ and C in the vicinity of critical temperatures, serving as indicators of the phase transitions. Overall, these findings suggest that For increasing field amplitudes (H), the transitions come about at lower temperatures.

Due to limited computational resources and time, a crude estimation of the transition temperatures is obtained from the locations of the peaks in $Var(Q_y)$ for different system sizes ($L=20, 30,$ and 40) with a fixed wavelength for both the cases (a) *Propagating wave* and (b) *Standing wave* ([Acharyya, 2018]). Remarkably, The peak positions remain consistent across different values of L , while the height of the peaks increases with higher L , indicating the development of critical correlations.

3.1.2 Comprehensive Phase Boundary

The dynamic transition temperatures in the system were influenced by the wavelength of the propagating magnetic field wave, while keeping the field amplitude fixed. Longer wavelengths of the propagating wave led to a transition from order to disorder at lower temperatures. A phase diagram was framed to represent the dependence of the non-equilibrium transition temperature on the maximum value of the magnetic field and wavelength of magnetic field. The phase boundaries were determined for different wavelengths, and it was observed that for longer wavelengths, the phase boundary contracted towards lower temperatures and field strengths Figure11(a). In contrast, the phase boundaries in the case of a standing magnetic wave Figure11(b) did not show a clear variation with wavelength. Further investigations are needed to better understand the behavior of the phase boundary in the case of a standing wave.

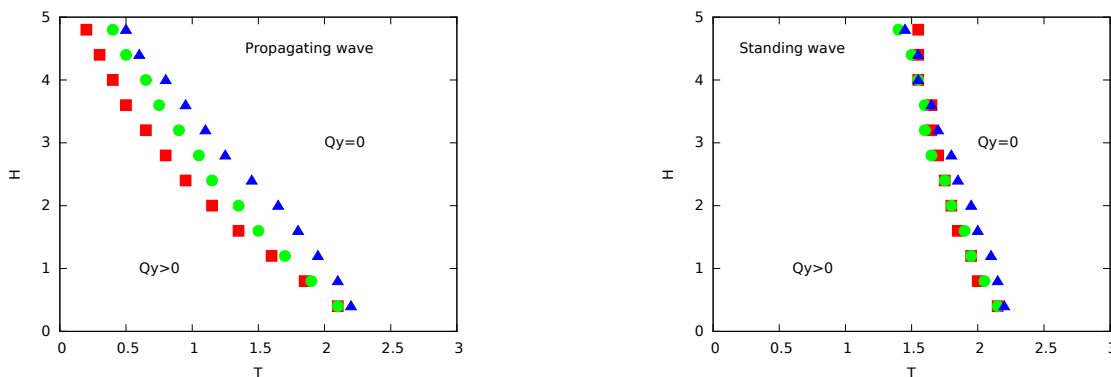


Figure 11: The sketch of phase separating lines for (a) Travelling wave and (b) Stationary wave. Different values of wavelengths λ are denoted by different symbols, $\lambda = 20$ (square), $\lambda = 10$ (bullet) and $\lambda = 5$ (triangle). Collected from [Acharyya, 2018]

A qualitative explanation for this observation can be offered by taking into account the wavelength as a gauge of the exposed region where spin flips occur. With a larger exposed area, lower temperature and weaker field intensity would be sufficient to generate dynamic order within the sample. However, this explanation is inadequate to fully understand the convoluted dependence of the phase separating line on wavelength in the case of a standing/stationary wave. Thus, additional research is needed to gain a deeper insight into this behavior of the phase boundary.

In the scenario of a stationary magnetic field wave, the dynamic phase at lower temperatures manifests as a stationary spin wave configuration. Such a nonequilibrium kind of transition with broken symmetry was observed, identical to the case of a travelling magnetic field wave,. The dynamic phase separating line was delineated, which displayed no significant reliance on the wavelength(λ) of the stationary field wave. Nevertheless, akin to the propagating wave case, the nonequilibrium transition temperature was found to converge toward the equilibrium transition temperature (approximately $2.20 J/k$) as the field amplitude approached zero, as reported by [Campostrini et al., 2001]. The nonequilibrium phase transition in the three-dimensional XY ferromagnet emerges due to the intricate interplay between the intrinsic time scale of the propagating magnetic field wave and the inherent relaxation time of the sample. As the ferromagnetic sample cools down from a hot thermal state, it progressively loses its ability to keep pace with the driving field, primarily due to an increasing intrinsic time scale. This leads to a lagging of phases between the system's response and the time-varying perturbation, ultimately resulting in dynamic

ordering. Since the field polarization aligns with the horizontal direction, the spin vector become unable to fully align with the field, causing the vertical component to possess a nonzero mean value while the horizontal component diminishes. Transitions occur at lower temperatures as the field intensity increases. The nonequilibrium effects arise from the contest between the distinct characteristics of the driving field and the inherent relaxation dynamics of the sample.

This research study extends an invitation to experimental researchers to explore the impact of dynamics of the spins in ferromagnetic polycrystals, such as compounds of Iron and Zinc. These materials can be effectively modeled as classical XY systems with diluted sites and superexchange interactions. Investigating the reaction and thermodynamic behavior of ferromagnetic samples under intensified optical environment holds significant relevance in the realm of spintronics. By conducting experiments on these systems, valuable insights can be gained into the dynamics and potential applications of ferromagnetic materials in spintronics research.

3.2 Anisotropic Heisenberg Ferromagnet in External Magnetic Field

When classical Heisenberg ferromagnetic system with anisotropy is perturbed by an external magnetic field, the Hamiltonian can be expressed as,

$$\mathcal{H} = -J \sum_{\langle ij \rangle} \vec{\sigma}_i \cdot \vec{\sigma}_j - D \sum_i (\sigma_i^z)^2 - \vec{h} \cdot \sum_i \vec{\sigma}_i \quad (10)$$

where $\vec{\sigma}_i$ represents a three dimensional classical spin vector of magnitude unity ($\sigma_{ix}^2 + \sigma_{iy}^2 + \sigma_{iz}^2 = 1$) quenched at the i -th lattice point of the sample. The three dimensional classical vector of the rotor, $\vec{\sigma}_i$ can assume any direction in the vector space. The exchange interaction term (the first term) describes the tendency of neighboring spins ($\langle ij \rangle$) to align with each other, with J representing the strength of this interaction. The second term accounts for the anisotropy energy, favoring spin alignment along the z -axis, with D indicating the strength of this anisotropy. It is pertinent to note here that when $D = 0$, the framework approaches to the isotropic Heisenberg limit, however as D grows to infinity, the system approaches the Ising limit. The third term (Zeeman term) depicts the system's interaction with an imposed time-varying magnetic field (\vec{h}). The field components vary sinusoidally in time, as defined by $h_\alpha = h_{0\alpha} \cos(\omega t)$, where $h_{0\alpha}$ denotes the amplitude having frequency f ($f = \omega/2\pi$).

Monte Carlo simulations were employed to study the described model. The equilibrium spin configuration at temperature T was obtained by gradually cooling the system from a random initial configuration. The simulations utilized the Metropolis algorithm with a random updating scheme. Further details on the simulation method can be found in standard textbooks. The simulations were performed on a 3D isometric sample with a linear system size of $L=20$, PBC were imposed in all of the three spatial directions. The α -th component of magnetisation at a time instant (per lattice site) is formulated as $m_\alpha(t) = \sum_i \frac{\sigma_\alpha^i}{L^3}$.

After integrating the simultaneous magnetization components across an entire cycle of the oscillation magnetic field, the steady value of the dynamical order-parameter components have been achieved: $Q_\alpha = \frac{1}{T} \oint m_\alpha(t) dt$. The vector addition of the three components provides the overall dynamical order parameter Q : $\vec{Q} = iQ_x + jQ_y + kQ_z$. Additionally, the instantaneous energy is given by the Hamiltonian (Equation-10). The time averaged energy is defined as the integrated Hamiltonian over an entire cycle of oscillation. The thermal gradient of energy (the specific heat) is defined as $C = \frac{dE}{dT}$ (calculated by three point central difference formula).

3.2.1 Longitudinal and transverse dynamic transition

Under the influence of a magnetic field that oscillates sinusoidally (with amplitude h_z^0 parallel to the anisotropy direction) an axial transition occurs in the dynamical order parameter component Q_z . At high temperature, the magnetic hysteresis loop ($m_z - h_z$) is symmetric, resulting in Q_z being zero. However, at low temperature, the loop becomes asymmetric, leading to a nonzero value of Q_z . Similar behavior is observed when a magnetic field is put orthogonal to the direction parallel to the anisotropy (x -direction), where the $m_z - h_x$ loop becomes asymmetric at low temperature while the $m_x - h_x$ loop remains symmetric. These transitions indicate a dynamic symmetry breaking from a symmetric to a symmetry broken phase as the temperature decreases. The off-axial transition is characterized by a 'marginally symmetric' behavior in the $m_z - h_x$ loop at higher temperatures, where the loop lies close to the h_x axis. This transition from 'marginally symmetric' to asymmetric occurs as the temperature decreases. Unlike longitudinal transitions, the transverse transitions are unable to revert the z -component of spin through the application of a field perpendicular to the anisotropy direction, resulting in a marginally symmetric loop. These observations highlight the importance of anisotropy for the occurrence of dynamic symmetry breaking within the framework of the conventional Heisenberg model in classical physics. [Acharyya, 2003].

To explore how the critical temperature relates the intensity of anisotropy (D) in both longitudinal type and transverse kind of transitions, the thermal dependence of the z component of dynamic order parameter (Q_z) was analyzed across various D values. In the axial transition case 12(a), it was found that at small values of D (for example, 0.5 and 2.5), the transition undergoes a discontinuous change, whereas at large values of D (such as 5.0 and 15), the transition occurs continuously. For the Ising limit ($D \rightarrow \infty$), the longitudinal transition was also observed and compared to the Ising model, showing a continuous transition occurring at a similar temperature. Similarly, in the off-axial transition 12(b), it was observed that the transition temperature moves towards higher values, with increasing D , and the nature of the transition is of continuous type for all anisotropy values. The comparison of the transition at $D = 400$ with the Ising model demonstrated their similarity in terms of a continuous transition occurring at approximately the same temperature. The effect of intensity of the anisotropy on the transition temperature, is attributed to how the anisotropy aligns the spin vector along its direction, requiring higher thermal fluctuations to break the symmetry. There is a distinction in the behavior of the transition between longitudinal and transverse scenarios, where the longitudinal transition demonstrates a discontinuous nature at comparatively smaller values of the anisotropy and develops into continuous for higher D values, while the transverse transition remains continuous throughout.

As the anisotropy approaches infinity, the characteristics or dynamics of the system differ depending on whether it is an axial or off-axial transition. When considering the scenario of longitudinal transition, the transition temperature in the Heisenberg ferromagnetic model with infinite anisotropy varies compared to that of the Ising model. Despite both models exhibiting the same transition temperature during equilibrium transitions, there is a disparity in the nonequilibrium transition temperatures. This is because the system remains in a nonequilibrium state due to the sinusoidally oscillating magnetic field applied in the z -direction, preventing it from becoming a conventional Ising system even when approaching the limit of enormously large anisotropy. In contrast, when it comes to transverse transitions, the critical temperatures in both the infinitely anisotropic Heisenberg ferromagnet and the Ising ferromagnet coincide perfectly. This is because the applied magnetic field, that oscillates sinusoidally in the x -direction, has no impact when anisotropy approaches to infinity. In this scenario, the infinitely anisotropic Heisenberg ferromag-

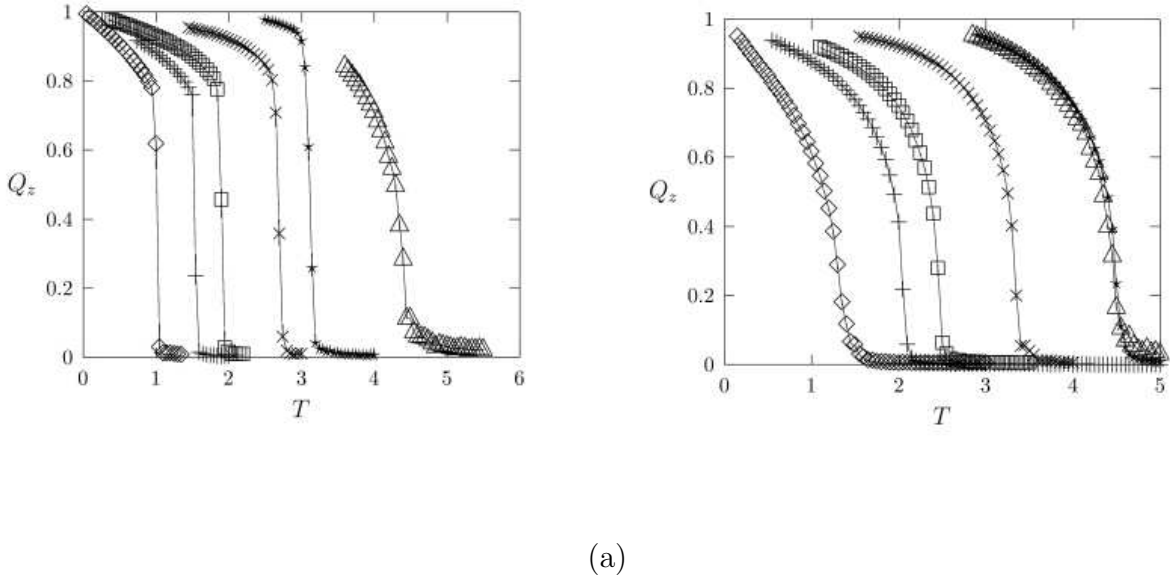


Figure 12: Thermal (T) dependence of the z component of the order parameter (Q_z) for various intensities of single site anisotropy (D): $D=0.50$ (diamond), $D=2.50$ (plus), $D=5.00$ (square), $D=15.00$ (cross) and $D=400$ (triangle). Figure(a) corresponds to axial ($h_z^0 = 0.50J$) dynamic transition and figure (b) corresponds to off-axial ($h_x^0 = 0.50J$) dynamic transition. For both the cases the thermal dependence of nonequilibrium ordering parameter in conventional Ising system (with $h_z^0 = 0.50J$ and $f = 0.001(MCSS)^{-1}$) are depicted by (star). Collected from [Acharyya, 2003].

net effectively maps onto the Ising ferromagnet in a state of statistical and thermal equilibrium when the field is perpendicular to the direction of easy axis. Consequently, the nonequilibrium transition in the Heisenberg model with infinite anisotropy perturbed by an transverse field and the equilibrium Ising ferromagnet in absence of applied magnetic field yield the identical results.

It is noteworthy to highlight a significant aspect concerning the dynamics employed in this simulation. Due to the non-commutation between the spin component and the Heisenberg Hamiltonian, the spin component displays inherent dynamics. This aspect was considered in a study that investigated the transport properties and the structure factor in the planar ferromagnet, highlighting the influence of the intrinsic dynamics on the system's behavior.

3.2.2 Elliptically polarized magnetic field: Multiple dynamic transition

If we consider an externally applied magnetic field that possesses elliptical polarization and is oriented within the X-Z plane, we can express this mathematically as follows;

$$\vec{h} = \hat{x}h_x + \hat{y}h_y + \hat{z}h_z = \hat{x}h_{0x}\cos(\omega t) + \hat{z}h_{0z}\sin(\omega t). \quad (11)$$

where,

$$\frac{h_x^2}{h_{0x}^2} + \frac{h_z^2}{h_{0z}^2} = 1, \quad (12)$$

Typically, h_{0x} and h_{0z} have different values. However, if we assume $h_{0x} = h_{0z} = h_0$, the magnetic field will exhibit circular polarization, satisfying the condition $h_x^2 + h_z^2 = h_0^2$. The externally

applied magnetic field and the intensity of anisotropy (D) are quantified in the units of J . The simulation method is implemented on an isometric 3D system with a linear size of $L = 20$ and employed PBC in each of 3 spatial dimensions.

The selection of the field amplitudes and frequency involved a meticulous search process to ensure their appropriateness for the study. The components of magnetic field amplitude were calibrated at $h_{0x} = 0.30$ and $h_{0z} = 1.00$. A frequency of $f = 0.02$ was chosen, leading to 50 MCSS encompassing one complete cycle which corresponds to the temporal period (τ) of the time varying magnetic field. The uniaxial anisotropy strength was chosen as $D = 0.2$, which remained constant throughout the investigation. It is worth noting that this specific value of D was prudently elected to ensure these intriguing results. However, diverse values of D are anticipated to lead to different transitions points and as D increases, the occurrence of multiple transitions is expected to diminish.

The dependency of the different components of the nonequilibrium ordering parameters (Q_α), upon the temperature, were investigated and illustrated in Figure 13(a). When the system undergoes gradually through a cooling process from a high temperature that corresponds to disordered ($\vec{Q} = 0$) state, first an intriguing transition occurs which corresponds to an *off axial* transition ([Acharyya, 2004]). The dynamical disordered phase denoted as ($\vec{Q} = 0, Q_x = 0, Q_y = 0, Q_z = 0$) shifts to a dynamical *Y ordered* phase (P1) specified by P1: ($Q_x = 0, Q_y \neq 0, Q_z = 0$) at critical temperature T_{c1} . The occurrence of an off-axial transition disrupts the dynamical symmetry of the system, specifically along the y direction. This disruption is a result of applying a magnetic field perpendicular to the preferred axis of order, which, in this case, confined in the plane formed by X and Z axes. When the sample undergoes through the cooling, it cherishes this specific non-equilibrium ordered phase (P1) over an appreciable temperature range. In the subsequent dynamic phase, denoted as P2, an *axial* transition occurs where the ordering characteristics change. Specifically, the components dynamic order-parameter are $Q_x \neq 0, Q_y = 0$ and $Q_z \neq 0$ and this transition takes place at a critical temperature T_{c2} . In phase P2, the system exhibits ordering in the plane defined by the applied magnetic field (X-Z plane), while the ordering across the Y direction diminishes. This transition signifies a shift in the dominant ordering behavior within the system. As the temperature continues to decrease, Q_x and Q_z progressively increase.

Upon reaching a specific temperature threshold (T_{c3}), another distinct transition occurs, manifesting a striking change in the system's ordering characteristics. In this newly emerged phase P3, the system undergoes a decline in X-ordering while the Z-ordering exhibits a rapid increase. Phase P3 is characterized by P3 : ($Q_x \neq 0, Q_y = 0, Q_z \neq 0$). Despite their apparent similarities in dynamic order parameter values, P2 and P3 exhibit a crucial distinction. In phase P2, the quantities Q_x and Q_z demonstrate an upward trend as temperature decreases, whereas in phase P3, Q_x exhibits a decline as temperature decreases (see Figure 13 (a)). These distinctions play a significant role in differentiating between the two phases. In phase P3, the system exhibits axial dynamical ordering along the Z-axis. As temperature decreases, the dynamical Z-ordering continues to increase. At very low temperatures, the system enters a phase with exclusive dynamic ordering along the Z-direction (where $Q_x = Q_y = 0$ and $Q_z = 1.0$), aligning with the direction of anisotropy.

The thermal dependence of the system's energy (E) is illustrated in Figure 13(b) to ascertain dynamic transitions and determine their corresponding transition temperatures. The plot clearly shows the three distinct dynamic transitions in this framework, characterized by arc points in the energy-temperature curve. The thermal gradient of energy yields the dynamical specific heat (C) which is graphically illustrated in Figure 13(c). The peak observed in the nonequilibrium specific

heat plot against temperature (C-T) curve evidently indicate the presence of the three dynamic transition. We can precisely measure the critical temperature by identifying the locus of the peaks: $T_{c1} = 1.22$ for first transition (P1), $T_{c2} = 0.94$ for the second transition (P2) and $T_{c3} = 0.86$ for the last one (P3).

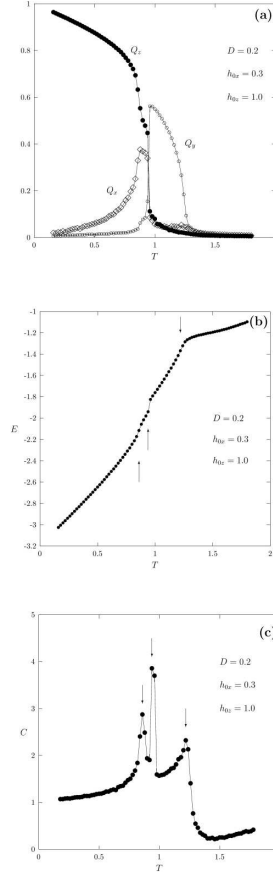


Figure 13: (a): The thermal variations of the dynamic order parameter components illustrated by distinct symbols Q_x (\diamond), Q_y (\circ) and Q_z (\bullet). The amount of the error during the measurement of Q_x , Q_y and Q_z near the critical point is approximately equal to 0.02 and that for the lower temperature (i.e., below $T = 0.50J/k_B$) is approximately equal to 0.003.;(b): The thermal dependence of the nonequilibrium energy. The critical points are pinned down by vertical arrows(c): The thermal dependence of dynamic specific heat ($C = \frac{dE}{dT}$). The vertical arrows indicate the position of critical points. These diagram are obtained for constant anisotropy $D = 0.20$ with elliptical polarisation having field amplitude $h_{0x} = 0.30$ and $h_{0z} = 1.00$. Collected from [Acharyya, 2004]

The scenario of multiple transitions evanesces for higher amplitude of field strength h_{0x} (while keeping the other parameters fixed). The C-T curve exhibits two peaks for $h_{0x} = 0.9$, indicating the presence of two distinct transitions. The second phase P_2 is no longer observed in this case. The system dynamically orders only along the direction of anisotropy (Z direction) and evidences a single transition for for $h_{0x} = h_{0z} = 0.2$ [circularly polarized; remaining all other parameter constant].

The system endures multiple dynamic phase transition for specific ranges of field amplitudes and for lower values of anisotropy. The Landau-Lifshitz-Gilbert equation accompanied by Langevin dynamics can be used to substantiate this phenomena. The synchronized rotation of spins may originate the multiple (longitudinal and transverse) dynamic transition in classical Heisenberg system having anisotropy. On the other hand in discrete model like Ising Model, the phenomena is commonly elucidated through the process of spin reversal and nucleation. However more detailed analysis are required to confirm the accountable reason for the appearance of multiple phases in non-equilibrium system.

The phase diagram, depicted in Figure. 14, exhibits the regions of different dynamic phases as a function of the applied field amplitude (h_{0x}) and temperature (T). Multiple dynamic transitions occur, giving rise to a complex phase landscape. In the Figure. 14, the superficial boundary separates the dynamically ordered phase (P_1 :Y ordered) specified by $Q_x = 0$, $Q_y \neq 0$, and $Q_z = 0$ from the disordered phase (P_0) characterized by $Q_x = 0$, $Q_y = 0$, and $Q_z = 0$. The transition temperature decreases with increasing field amplitude (h_{0x}). For small values of h_{0x} , a distinct region confined by the symbols circle and bullet corresponds to the ordered phase denoted as P_2 . In this phase, $Q_x \neq 0$, $Q_y = 0$, and $Q_z \neq 0$. Although this region is small in area, it is clearly observed and carefully analyzed. As the field amplitude h_{0x} grows, the transition temperatures for both extends of this phase drop.

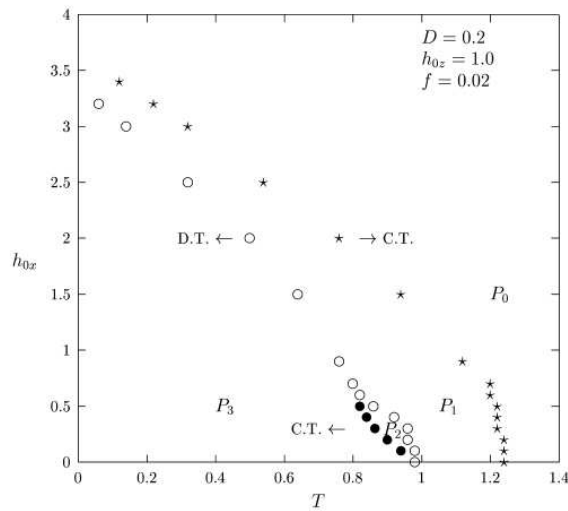


Figure 14: The phase diagram illustrates nonequilibrium multiphasal transitions in the $T - h_{0x}$ plane for parameters $D=0.2$, $f=0.02$, and $h_{0z}=1.0$. The diagram distinguishes between continuous transitions (C.T.) and discontinuous transitions (D.T.) across the phase separating lines, indicating the nature of the transitions. Collected from [Acharyya, 2005]

The region inside the phase plane, bounded by both the circle (representing large h_{0x} values)

and the bullet (representing small h_{0x} values), corresponds to the low-temperature phase labeled as P_3 . In this phase, Q_x and Q_y are zero, while Q_z is non-zero. Analogous to the other phases, the transition temperature exhibits a reduction with an increase in the field amplitude h_{0x} . The obtained phase diagram provides valuable insights into the complex behavior of the system under varying temperatures and applied field amplitudes. The different dynamic phases and their boundaries offer a comprehensive understanding of the interplay between temperature, field amplitude, and the resulting magnetization patterns.

The study investigates the nature of multiple dynamic transitions in a system by analyzing the distributions of dynamic order parameter components near the transition points. The transitions are examined in a phase portrait confined in the $h_{0x} - T$ plane. The transition from the high temperature structureless phase (P_0) to the Y -ordered phase (P_1) is found to be continuous. The distribution of Q_y shifts gradually towards zero as the temperature increases, indicating a continuous transition at around $T = 1.20$. In contrast, the transition from P_1 to P_3 is discontinuous. As the temperature decreases, the value of Q_y drops abruptly from a nonzero value to zero. The distribution of Q_y exhibits two peaks near the transition temperature ($T \approx 0.79$), indicating a discontinuous transition. The transition from P_2 to P_3 is found to be continuous, with the value of Q_z changing smoothly. The Binder cumulant ratio U_y confirms these findings, showing a monotonic change for the continuous transition and a sharp minimum for the discontinuous transition. The nature of the transitions is summarized in a phase diagram, providing a comprehensive representation of the system's dynamic behavior.

The study also highlights the importance of choosing appropriate field amplitudes for accurate analysis. The chosen value of $h_{0x} = 0.7$ allows for well-separated phase boundaries, facilitating the examination of temperature variations. Furthermore, the analysis of the distribution of Q_z near the transition from P_2 to P_3 proves challenging due to the small change in Q_z . However, the thermal dependence of the Binder cumulant ratio U_z shows a smooth variation, indicating a continuous transition.

Overall, the results demonstrate the existence of both continuous and discontinuous transitions in the system. The study provides valuable insights into the dynamic behavior and nature of these transitions, contributing to a better understanding of complex systems. Further investigations, including larger system sizes and precise estimation of transition temperatures, are suggested to study scaling behavior and critical exponents associated with these transitions.

The findings of a finite size study conducted and briefly documented [Acharyya, 2005] suggest that the observed multiple non-equilibrium transitions presented earlier are unlikely to be a result of finite size effects.

The thermal dependence of the variances of the non-equilibrium order parameter components (Q_x, Q_y, Q_z) for various system sizes are studied. The results show that the variances exhibit sharp peaks at the transition temperatures (T_{c1} and T_{c2}) corresponding to the dynamic phase transitions. The height of the peaks increases with larger system sizes, indicating the presence of a diverging length scale at the transition points. The study also suggests that the transition temperature (T_{c3}) for the transition from P_2 to P_3 phase cannot be resolved from the present analysis. The error bars in the components of the ordering parameters show maximum growth in the vicinity of T_{c1} and T_{c2} , while the behavior near T_{c3} is less clear. These findings provide valuable insights into the dynamic behavior of the system and highlight the importance of system size in understanding the transition phenomena.

A brief investigation was conducted on the frequency dependence of the multiphase nonequilibrium transitions. The thermal dependence of the components of the non-equilibrium order parameter are studied for a small frequency ($f = 0.01(MCSS)^{-1}$) of the polarized magnetic field,

the transitions were studied under the conditions of $D = 0.20J$, $h_{0x} = 0.30J$, and $h_{0z} = 1.0J$. Similar temperature trends were observed compared to the $f = 0.02(MCSS)^{-1}$ case ($D = 0.2J$, $h_{0x} = 0.3J$, and $h_{0z} = 1.0J$), albeit with a noticeable shift of the critical points towards lower temperatures. By examining the thermal variations of the $\frac{dQ_x}{dT}$, $\frac{dQ_y}{dT}$, and $\frac{dQ_z}{dT}$, the approximate values of $T_{c1} \simeq 1.06$, $T_{c2} \simeq 0.76$, and $T_{c3} \simeq 0.62$ were obtained. A similar analysis was performed for comparatively a large values of $h_{0x}(= 1.5)$ assuming $f = 0.01$, $D = 0.2$, and $h_{0z} = 1.0$. In this scenario, only two transitions were obtained, and the estimated critical temperatures were $T_{c1} \simeq 0.60$ and $T_{c3} \simeq 0.30$. These investigations provide evidence that as the frequency decreases, approaching the equilibrium limit, the critical points in the phase diagram shift towards lower temperatures while maintaining the general structure of the diagram unchanged (for $f = 0.02$). This observation aligns with the expectation that at lower frequencies, the magnetization components have more time to align with the field, resulting in the disappearance of the dynamic transition. Hence, this transition is referred to as a "truly dynamic" transition.

What will be the responses of a needle like nanomagnet to the electromagnetic (EM) radiation passing through it? To study such kind of nonequilibrium responses, the needle like anisotropic Heisenberg ferromagnet irradiated by the propagating electromagnetic field wave has been studied by standard MC simulation using Metropolis rate of single spin-flip. The electromagnetic wave has been considered to propagate through the z-axis (easy axis here). The needle was found to show a nonequilibrium kind of phase transition at a finite critical temperature where time averaged magnetisation over the full cycle of the propagating radiation assumes nonzero value in the low temperature ordered phase.

The comprehensive phase diagram has been shown in the Euclidian plane formed by the critical temperature and the maximum magnitude of the spatio-temporal variation of the propagating magnetic field wave. The following figure (Fig-15) shows the comprehensive phase diagram.

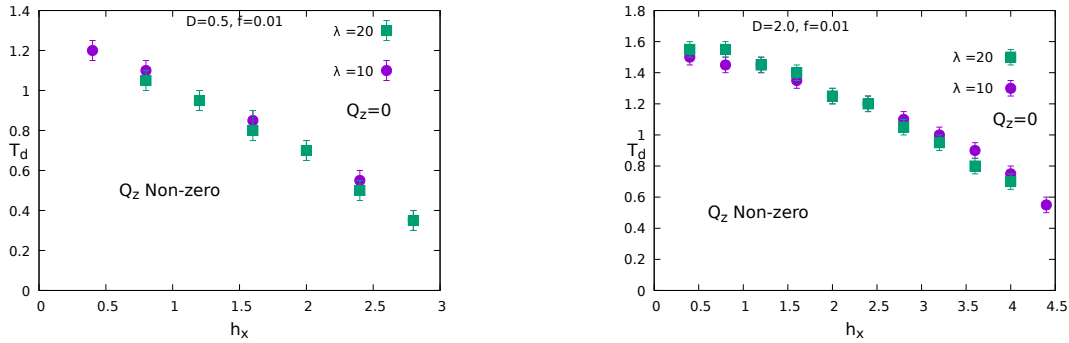


Figure 15: The phase separating boundaries for the phase transition of nonequilibrium type in rodlike Heisenberg ferromagnet for different anisotropies ($d = 0.5$ (left) and $D = 2.0$ (right)) Different symbols represent wavelengths (λ) of different values of travelling magnetic field wave. Collected from [Acharya, 2022]

4 Technological significance:

Magnetism has taken an important place in modern technology. Magnetic force is one of the most fundamental forces in the universe and has been used by mankind for thousands of years. The magnetic memory device is the most common example of the use of magnetic materials. In present days, the great challenge is to design such a memory or recording device which maximizes the storage capacity and recording speed. To develop such materials one should have adequate knowledge about its magnetic properties along with the thermodynamical behaviours. Theoreticians play the significant role to understand the various thermodynamic phases through model calculations. The computer simulation studies help to predict the behaviours in the limiting points. Moreover, the microscopic configuration or the morphological structures of magnetic materials, can be visualised through the computer simulation of such classical vector (spin) models.

The magnetic materials having very large values of magnetic moments can be a special representation of classical spin vectors. These kinds of materials can be used in *magnetic coating* devices. These devices are operationally active in specially designed optically sensitive domain. The low temperature behaviours of such systems can be a realisation of classical Heisenberg or planar ferromagnet irradiated by electromagnetic field wave. The domain of maximal activity may be searched in the symmetry broken dynamically ordered phase as described in Section-3. Moreover, the widely used SMOKE (Surface magneto optic Kerr effect) can be employed to study the effective change in the magnetisation in the dynamically symmetric phase, which may help to identify the maximally active domain as stated above.

5 Summary:

It should be mentioned here that this article is mainly reviewed the equilibrium and nonequilibrium phase transitions studied in classical XY and Heisenberg models. The quantum behaviour of these models show many interesting behaviours which is beyond the scope of present article. The interested reader may consult the book [Sachdev, 2000] Quantum Phase Transitions by Subir Sachdev. The quantum phase transitions [Dutta et al., 2015] are mainly studied by tuning the transverse field. The thermodynamic behaviours of such magnetic models are not the main goal of such studies.

The thermodynamic behaviours of classical XY and Heisenberg model are briefly reviewed here. In this view, the interested reader may get all necessary up-to-date informations in this review article. Some recent studies are also included here. The main systems of review are XY model and Heisenberg model. The whole article is mainly divided in two parts: the equilibrium behaviours and the nonequilibrium behaviours. The nonequilibrium behaviours are modelled by the time dependence of the generic Hamiltonian through a time dependent externally applied magnetic field. On the other hand the equilibrium behaviours are thoroughly reviewed on the basis of the roles of anisotropy, dilution as the effects of disorder.

In the study of equilibrium type of phase transitions, the dependences of the critical temperatures on the amount of disorder (anisotropy, dilution etc.) has been discussed with recent developments. The quantum and classical calculations are discussed in this context. In some cases, the distributed anisotropy was found to play a pertinent role in determining the critical temperature. The most recent results are discussed in details. The thermodynamics behaviours of metamagnets (layered antiferromagnets), modelled by classical XY and Heisenberg systems, are also discussed (with phase diagrams) in this article. In some cases, for completeness, the

experimental results and the theoretical results are compared with reasonable agreement.

On the other hand, nonequilibrium phase transitions in XY and Heisenberg ferromagnets, investigated in last two decades, have been discussed in details. The nonequilibrium phase transitions, in such systems, driven by oscillating, propagating, polarised magnetic fields are discussed. The nonequilibrium phase transition in XY nanorod is also analysed.

A section (section-3) has been devoted here to the technological significance of such theoretical studies. Basically, the metamagnetic behaviours of such systems (In FeBr_2) have been successfully modelled by Heisenberg metamagnets. The rich phase diagram of such systems may be employed to design magnetic materials for interesting magnetocaloric effects..

Lastly, we believe that this review is a modern documentation of the thermodynamic behaviours and ordering of various magnetic systems which can be modelled by classical XY and Heisenberg ferromagnets. This will be useful for the modern research in the field of thermodynamics of magnetism and its statistical aspects in the context of quenched disorder.

6 Acknowledgements:

The MANF, UGC, Govt. of India is gratefully acknowledged by Olivia Mallick for financial support. Muktish Acharyya thankfully acknowledges FRPDF, Presidency University. Collaborations with Ulrich Nowak, Klaus Usadel and Erol Vatansever are gratefully acknowledged. We acknowledge Ishita Tikader for a careful reading of the manuscript. We sincerely thank Dr. Anuj Bhowmick for his kind help in preparing the manuscript.

References

- [Acharyya, 2003] Acharyya, M. (2003). Axial and off-axial dynamic transitions in uniaxially anisotropic heisenberg ferromagnet: A comparison. *International Journal of Modern Physics C*, 14.
- [Acharyya, 2004] Acharyya, M. (2004). Multiple dynamic transitions in an anisotropic heisenberg ferromagnet driven by polarized magnetic field. *Phys. Rev. E*, 69:027105.
- [Acharyya, 2005] Acharyya, M. (2005). Nonequilibrium multicritical behavior in anisotropic heisenberg ferromagnet driven by oscillating magnetic field. *Int. J. Mod. Phys. C*, vol-17.
- [Acharyya, 2018] Acharyya, M. (2018). Driven spin wave modes in xy ferromagnet: non-equilibrium phase transition. *Phase Transitions*, 91(8):793–810.
- [Acharyya, 2022] Acharyya, M. (2022). Rodlike heisenberg nanomagnet driven by propagating magnetic field: Nonequilibrium phase transition. *International Journal of Modern Physics C*, 33(10).
- [Acharyya et al., 2000] Acharyya, M., Nowak, U., and Usadel, K. D. (2000). Transverse ordering of an antiferromagnet in a field with oblique angle to the easy axis. *Phys. Rev. B*, 61:464–469.
- [Acharyya and Vatansever, 2022] Acharyya, M. and Vatansever, E. (2022). Monte carlo study of the phase diagram of layered xy antiferromagnet. *Physica A: Statistical Mechanics and its Applications*, 605:128018.

- [Agrawal et al., 2021] Agrawal, R., Kumar, M., and Puri, S. (2021). Domain growth and aging in the random field xy model: A monte carlo study. *Phys. Rev. E*, 104:044123.
- [Akgenc et al., 2021] Akgenc, B., Vatansever, E., and Ersan, F. (2021). Tuning of electronic structure, magnetic phase, and transition temperature in two-dimensional cr-based janus mxenes. *Phys. Rev. Mater.*, 5:083403.
- [Berger et al., 2013] Berger, A., Idigoras, O., and Vavassori, P. (2013). Transient behavior of the dynamically ordered phase in uniaxial cobalt films. *Phys. Rev. Lett.*, 111:190602.
- [Betts and Lee, 1968] Betts, D. D. and Lee, M. H. (1968). Critical properties of the XY model. *Phys. Rev. Lett.*, 20:1507–1510.
- [Bilican et al., 2023] Bilican, F., Ozdemir Kart, S., Vatansever, E., Ersan, F., and Demir Vatansever, Z. (2023). Strain effects on the electronic and magnetic properties of Cr₂TaC₂ and Cr₂TaC₂O₂ monolayers. *Applied Physics Letters*, 122(15):151901.
- [Binder and Landau, 1976] Binder, K. and Landau, D. P. (1976). Critical properties of the two-dimensional anisotropic heisenberg model. *Phys. Rev. B*, 13:1140–1155.
- [Campostrini et al., 2001] Campostrini, M., Hasenbusch, M., Pelissetto, A., Rossi, P., and Vicari, E. (2001). Critical behavior of the three-dimensional xy universality class. *Physical Review B*, 63(21):214503.
- [DeFotis et al., 2008] DeFotis, G. C., Huddleston, R. A., Rothermel, B. R., Boyle, J. H., Vos, E. S., Matsuyama, Y., Hopkinson, A. T., Owens, T. M., and May, W. M. (2008). Dependence of the magnetic ordering temperature on dilution in a 3d xy insulating ferromagnet. *Journal of Physics: Condensed Matter*, 20(13):135222.
- [Dutta et al., 2015] Dutta, A., Aeppli, G., Chakrabarti, B., Divakaran, U., Rosenbaum, T., and Sen, D. (2015). *Quantum phase transitions in transverse field spin models: From statistical physics to quantum information*, volume 653. Cambridge University Press.
- [Flax, 1970] Flax, L. (1970). *Theory of the Anisotropic Heisenberg Ferromagnet*. National Aeronautics and Space Administration.
- [Freire and Plascak, 2015] Freire, R. T. S. and Plascak, J. A. (2015). Bicritical universality of the anisotropic heisenberg model in a crystal field. *Phys. Rev. E*, 91:032146.
- [Fröhlich and Lieb, 1977] Fröhlich, J. and Lieb, E. H. (1977). Existence of phase transitions for anisotropic heisenberg models. *Phys. Rev. Lett.*, 38:440–442.
- [Hasenbusch, 2008] Hasenbusch, M. (2008). A monte carlo study of the three-dimensional xy universality class: universal amplitude ratios. *Journal of Statistical Mechanics: Theory and Experiment*, 2008(12):P12006.
- [Kanbur et al., 2020a] Kanbur, U., Polat, H., and Vatansever, E. (2020a). Thermal properties of rung-disordered two-leg quantum spin ladders: Quantum monte carlo study. *Phys. Rev. E*, 102:042104.
- [Kanbur et al., 2020b] Kanbur, U., Vatansever, E., and Polat, H. (2020b). Universality in the three-dimensional random bond quantum heisenberg antiferromagnet. *Phys. Rev. B*, 102:064411.

- [Kosterlitz, 1974] Kosterlitz, J. M. (1974). The critical properties of the two-dimensional xy model. *Journal of Physics C: Solid State Physics*, 7(6):1046.
- [Lach and Žukovič, 2020] Lach, M. and Žukovič, M. (2020). New ordered phase in geometrically frustrated generalized xy model. *Phys. Rev. E*, 102:032113.
- [Lach and Žukovič, 2021] Lach, M. and Žukovič, M. (2021). Phase diagrams of the antiferromagnetic xy model on a triangular lattice with higher-order interactions. *Phys. Rev. E*, 104:024134.
- [Ma and Figueiredo, 1997] Ma, Y.-q. and Figueiredo, W. (1997). Phase diagram of the anisotropic xy model. *Phys. Rev. B*, 55:5604–5607.
- [Mallick and Acharyya, 2022] Mallick, O. and Acharyya, M. (2022). Critical behaviours of anisotropic and impure xy ferromagnets. *arXiv preprint arXiv:2208.10109*.
- [Mallick and Acharyya, 2023] Mallick, O. and Acharyya, M. (2023). Critical behaviours of anisotropic xy ferromagnet in the presence of random field. *arXiv preprint arXiv:2306.02162*.
- [Mubayi and Lange, 1969] Mubayi, V. and Lange, R. V. (1969). Phase transition in the two-dimensional heisenberg ferromagnet. *Phys. Rev.*, 178:882–894.
- [Naskar et al., 2023] Naskar, M., Acharyya, M., Vatansever, E., and Fytas, N. G. (2023). Disorder effects on the metastability of classical heisenberg ferromagnets. *Physical Review E*, 108(1).
- [Oguchi, 1971] Oguchi, A. (1971). Phase Transition of the Heisenberg Ferromagnet. *Progress of Theoretical Physics*, 46(1):63–76.
- [Petracic et al., 1998] Petracic, O., Binek, C., Kleemann, W., Neuhausen, U., and Lueken, H. (1998). Field-induced transverse spin ordering in febr 2. *Physical Review B*, 57(18):R11051.
- [Rapini et al., 2007] Rapini, M., Dias, R. A., and Costa, B. V. (2007). Phase transition in ultrathin magnetic films with long-range interactions: Monte carlo simulation of the anisotropic heisenberg model. *Phys. Rev. B*, 75:014425.
- [Riego et al., 2017] Riego, P., Vavassori, P., and Berger, A. (2017). Metamagnetic anomalies near dynamic phase transitions. *Phys. Rev. Lett.*, 118:117202.
- [Sachdev, 2000] Sachdev, S. (2000). *Frontmatter*, pages i–vi. Cambridge University Press.
- [Santos-Filho and Plascak, 2011] Santos-Filho, J. and Plascak, J. (2011). Monte carlo simulations of the site-diluted three-dimensional xy model. *Computer Physics Communications*, 182(5):1130–1133.
- [Serena et al., 1993] Serena, P. A., Garcí'a, N., and Levanyuk, A. (1993). Monte carlo calculations on the two-dimensional anisotropic heisenberg model. *Phys. Rev. B*, 47:5027–5036.
- [Shenoy and Chattopadhyay, 1995] Shenoy, S. R. and Chattopadhyay, B. (1995). Anisotropic three-dimensional xy model and vortex-loop scaling. *Phys. Rev. B*, 51:9129–9147.
- [Siurakshina et al., 2000] Siurakshina, L., Ihle, D., and Hayn, R. (2000). Theory of magnetic order in the three-dimensional spatially anisotropic heisenberg model. *Phys. Rev. B*, 61:14601–14606.

- [Stanley and Kaplan, 1966] Stanley, H. E. and Kaplan, T. A. (1966). Possibility of a phase transition for the two-dimensional heisenberg model. *Phys. Rev. Lett.*, 17:913–915.
- [Su et al., 2022] Su, Y., Liu, D., Wan, Z., Chen, A., and Cheng, P. (2022). Quantum criticality in spin-1/2 anisotropic xy model with staggered dzyaloshinskii–moriya interaction. *Physica A: Statistical Mechanics and its Applications*, 594.
- [Zucker, 2011] Zucker, I. (2011). 70+ years of the watson integrals. *Journal of Statistical Physics*, 145:591–612.